PERGAMON

International Journal of Heat and Mass Transfer 43 (2000) 251–262

International Journal of HEAT and MASS TRANSFER

www.elsevier.com/locate/ijhmt

Fluid flow and heat transfer over straight and curved rough surfaces

A.B. Turner*, S.E. Hubbe-Walker, F.J. Bayley

Thermo-Fluid Mechanics Research Centre, School of Engineering, University of Sussex, Brighton, UK

Received 9 October 1998; received in revised form 6 April 1999

Abstract

Measurements of fluid pressure, velocity, including turbulent fluctuations and heat transfer were made over the straight and curved lower surface of a wind tunnel with an upper surface which could be flexed to control the streamwise pressure gradients. Laser–Doppler techniques were employed for flow visualisation and detailed investigation of the flow structure. These were roughened in a structured manner with machined excrescences of pyramidal and trapezoidal shape. Fluid dynamic data are presented for smooth and rough surfaces and heat transfer results from roughnesses of three different heights. Velocity gradients and curvature, less than often found in turbo-machinery, in the ranges examined, had relatively little effect compared to the roughness. The present observations are compared with relevant data in the literature. The elements of the present work showed enhancement of heat transfer at comparable conditions over 70% more than the more commonly reported spherical forms. The observations are also compared with the predictions of a computational fluid dynamic procedure developed in the authors' laboratory (F.H.A. Tarada, Heat transfer to rough turbine blading. University of Sussex, D.Phil thesis, 1987) with which there is fair to good agreement. Although the code overpredicts the effects of surface curvature and pressure gradients, and the level of heat transfer at the higher velocities, discrepancies are usually within the experimental uncertainties. The comprehensive range of fluid dynamic and heat transfer results are presented by Hubbe-Walker (S.E. Hubbe-Walker, An experimental study of the effects of roughness and curvature on heat transfer in turbulent boundary layers. University of Sussex, D.Phil. thesis, 1996), is intended to provide a database for the development of more recent analytical and CFD procedures.

Keywords: Heat transfer measurements; Rough surfaces; LDA profiles; Numerical predictions

1. Introduction

Modern gas turbines almost universally employ cooling systems for the high-pressure turbine blades. Accurate prediction of the operating lives of these critical components requires reliable values of the heat transfer rates in the design stage of the system. On the coolant side, where complex internal geometries are used, empirically derived heat transfer coefficients can be employed with confidence by the designer. On the hot gas side of the system, where the fluid stream is often unsteady and subject to artificially high turbulence levels, computational fluid dynamics (CFD) techniques have found considerable application in optimising aerodynamic stage design and to a less extent in predicting heat transfer rates. In practice, the

* Corresponding author. Tel.: +44-1273-606755; fax: +44-1273-678335.

0017-9310/00/$ - see front matter
PII: S0017-9310(99)00128-3

Nomenclature

blt	boundary layer thickness, defined at $U/U_s = 0.99$	St	Stanton number, $h/\rho U C_p$
C_p	specific heat capacity	Tu	turbulence intensity, $u'v'/U^2$
De	Dean number, $(U_s H/\nu)\sqrt{(H/R)}$	U	velocity
e	ramping factor	U_τ	friction velocity, $\sqrt{(u'v')}$
h	heat transfer coefficient	U_s	mainstream velocity
H	tunnel height	U	U/U_τ
K	specific kinetic energy of turbulence	u'	fluctuating component of U
K_r	roughness acceleration parameter, $(k_r/U_s)\,\mathrm{d}U_s/\mathrm{d}x$	v'	transverse velocity fluctuation
		x	distance along tunnel
k_r	roughness height	y	distance into flow
k_s	equivalent sand roughness height	y^*	yU^*/ν
Pr	Prandtl number, $\mu C_p/\lambda$	ε	kinetic energy dissipation
R	radius of curvature	λ	thermal conductivity
Re	Reynolds number, $\rho U x/\mu$	ρ	density
Re_k	roughness Reynolds number, $k_r U_\tau/\nu$	μ	dynamic viscosity
		ν	kinematic viscosity, μ/ρ

operational fluid flow conditions restrict the confidence that can be placed in such predictions and, in particular, for the consequences of changes in the nature of the surface swept by the hot gases, which raise problems that have been little considered in the literature. Fig. 1 shows a high-pressure blade from a marine gas turbine after 3,500 h of operation, in which, the roughness of the surface due to erosion and oxidation is clearly apparent. The effect of such a condition is a fluid dynamic phenomenon that has been long appreciated and constantly investigated since Nikuradse's systematic and classical work in the early years of the present century [2]. Such work has, however, been generally concerned with steady flows in pipes and little attention has been given to the effects of surface roughness on curved flows in streamwise pressure gradients which are usual in turbo-machinery. Roughness is known to reduce significantly the performance of turbine blading, with possibly contradictory aerodynamic and thermodynamic consequences as demonstrated by Turner et al. [3].

A theoretical analysis was developed by Tarada [1,4], specifically to predict flows and heat transfer over rough surfaces. He employed a low Reynolds number turbulence model similar to that developed by Jones and Launder [5], supplemented by an algebraic stress model for curved boundary layer flow with the surface roughness modelled topographically. The object of the programme reported in this paper has been to make detailed and accurate measurements of the flow and heat transfer over a surface with the characteristics considered by Tarada. The results

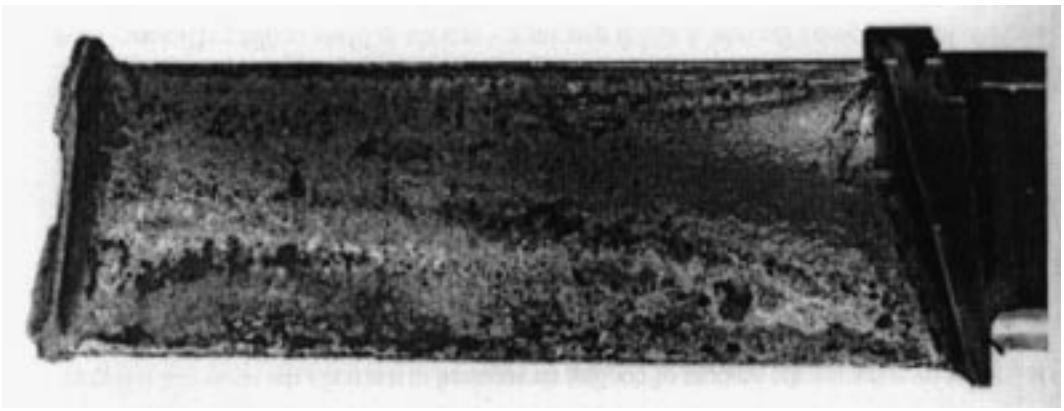

Fig. 1. Eroded turbine blade.

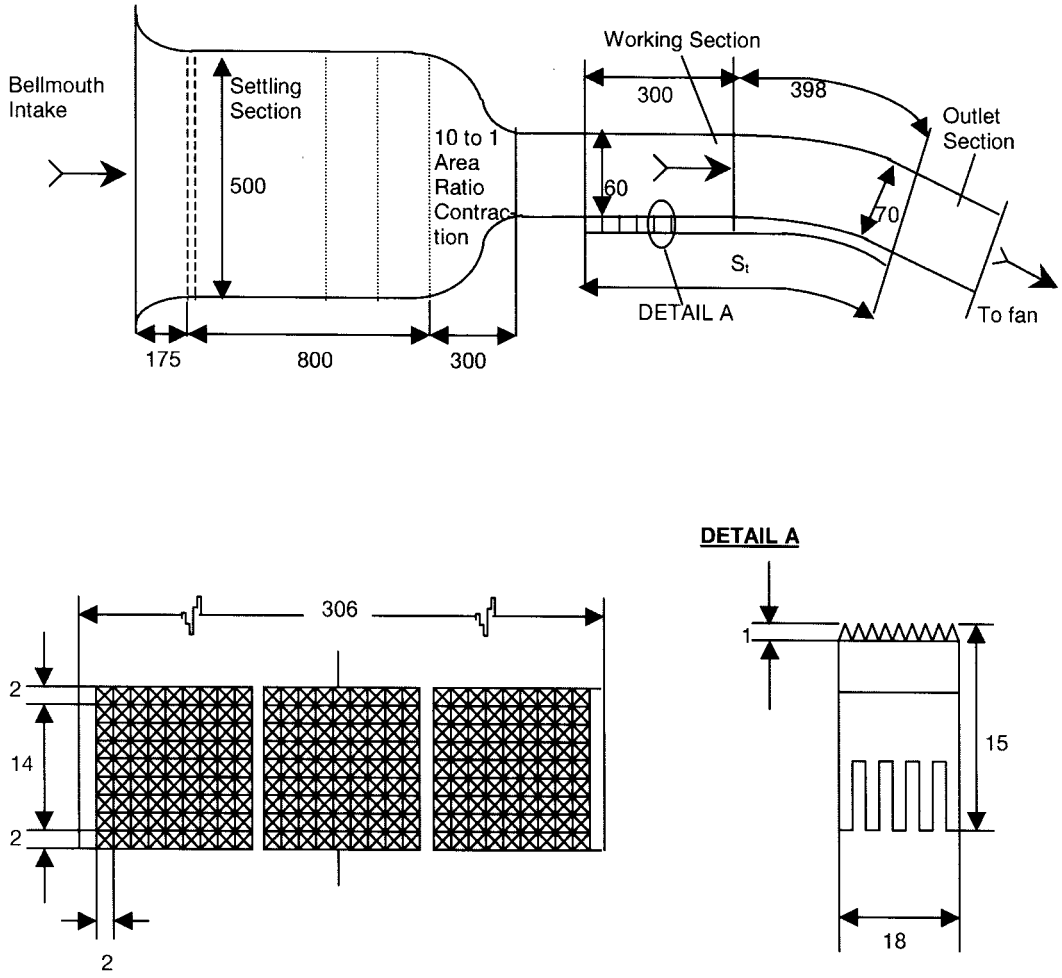

Fig. 2. Experimental apparatus.

obtained are used to compare predictions from his theory and to establish a database for comparison with later relevant theoretical analyses.

2. Experimental apparatus

The general arrangement of the wind tunnel used for the present experimental programme is shown as Fig. 2. Air was drawn by a centrifugal blower through a bell-mouth intake and settling section into a convergent entry duct followed by an inlet length before the working section. Transparent side-walls allowed access to the working region for laser–Doppler measurements and for the high speed camera used briefly to follow the development of the flow in the working section. The top was flexible to control the velocity and pressure gradients in the working section, which was rectangular in cross-section, 300 mm wide and 70 mm high with a straight section of 300 mm. This was followed by a curved section of radius 1.2 m over an arc of 19° and extending for another 400 mm. The inlet length of 160 mm incorporated a suction slot connected to a plenum chamber through which the boundary layer could be drawn off with an auxiliary centrifugal blower.

The floor of the tunnel was constructed from 40 aluminium alloy bars, 300 mm long to correspond to the tunnel width, 15 mm deep and measuring 18 mm in the direction of flow. The surface topography was a regular array of elements, initially pyramidal 1 mm high, formed using a single point cutter to machine grooves orthogonally along and across each bar. This operation produced a series of elements arranged in a square configuration on a base of 2 mm, the tops of which were later successively milled down to 0.75 and

then 0.5 mm high trapezoidal sections. To maintain uniformity of element pitching, insulating spacing strips were included between each separate bar to facilitate control of the surface temperature distribution in the heat transfer tests.

For these tests, electric current was supplied to electrically insulated heater wires in slots machined into the back of each bar as shown in Fig. 2. Surface temperature measurements were made with resistance-temperature matched thermistor beads inserted to within 3 mm of the surface in blind holes on the tunnel spanwise centre-line. For comparative purposes, type K nickel–chromium/nickel–aluminium thermocouple beads were used in eight of the roughness bars.

Velocity measurements in the working section were made using either a standard hook shaped pitot probe traversed from the top surface in conjunction with static pressure tappings in the surface. Laser–Doppler anemometry (LDA) available for part of the programme was employed through the side tunnel walls. This comprised a 4 W Argon-ion laser with associated transmitting optics that produced two parallel beams of equal intensity arranged to intersect in the flow, which was seeded from a smoke generator. The receiving optics comprised a photo detector, a photomultiplier assembly and a Doppler frequency counter. Fringe spacing in the intersecting area and its effect in modulating the light intensity at an observed frequency, provided a measure of mainstream velocity. A traversing bench driven by stepper motors allowed measurements at frequent close spacing through the flow. This could position the light beam with an accuracy estimated at 0.05 mm and with an intersection probe volume produced by the transmitter optics calculated to be 0.207 mm in diameter by 3.063 mm long with a fringe spacing of 3.61 μm.

The LDA system could also be used for flow visualisation in the seeded fluid stream. A cylindrical lens and Schlieren mirror in the transmission optics produced a sheet of light in the flow approximately 1 mm thick that enabled the flow structure to be observed throughout the test section.

3. Experimental observations

3.1. General

The complete experimental programme consisted, first, of flow visualisation, LDA and pitot probe velocity measurements over unheated rough surfaces with the roughness elements 1 mm high on the 300 mm long straight and 400 mm curved test sections. Traverses were made over the whole tunnel height at six stations down the complete tunnel and at five mainstream velocities from 17 to 40 m/s. Comparable smooth surface tests were also conducted with a flat thin steel sheet covering the roughness.

Second, heat transfer tests were made using only the pitot tube for velocities but with 3° of surface roughness, corresponding to the original 1 mm elements cut back successively to heights of 0.75 and 0.5 mm.

Flow visualisation showed that a step effect from the suction slot in the floor of the tunnel inlet section was causing boundary layer separation at the start of the working section. This part of the program was thus used principally to determine the suction rate through the plenum chamber to optimise the flow at the entrance to the test section, with just no separation. The visualisation also showed clearly that an obviously turbulent boundary layer occurred ab initio over the rough surfaces whereas, there was an obvious laminar–turbulent transition over the smooth surface, as shown in Fig. 3a and b, in which, the flow is from right to left.

3.2. Fluid flow

Fig. 4 compares conditions through the boundary layers towards the downstream end of the straight working section for the rough and smooth surfaces where the corresponding mainstream Reynolds number is about 5×10^6.

Fig. 4 demonstrates the greater velocity deficit caused by the roughness: the index $1/n$, used traditionally to represent the velocity distribution in a boundary layer, is for the rough surface, about 1/2.65. The equivalent plot for the smooth wall corresponds to a boundary layer index of about 1/5.3. The enhanced turbulence intensity near the rough wall surface is also clear.

In the tests, measurements were made of the longitudinal and transverse components of velocity fluctuation by yawing the laser beam splitter and measuring the mean and root mean square values of the velocity vectors at three different angular positions, according to the methods developed by Tropea [6]. The inferred velocity perturbations were not, however, reliable on the rough surface because of regions of local three-dimensional flow located very near the roughness elements. These include small regions of separated flow behind the individual elements, and strong mixing and high turbulence just above. The consequent scattering of laser light prevented the acquisition of reliable measurements in parts of these regions. For comparative purposes, however, in Fig. 5 are plotted a selection of the readings of Reynolds shear stress measurements through the boundary layers on the smooth and rough walls.

Fig. 6 shows the corresponding non-dimensional plots of the velocity distribution over the smooth and rough walls, from the LDA measurements of the

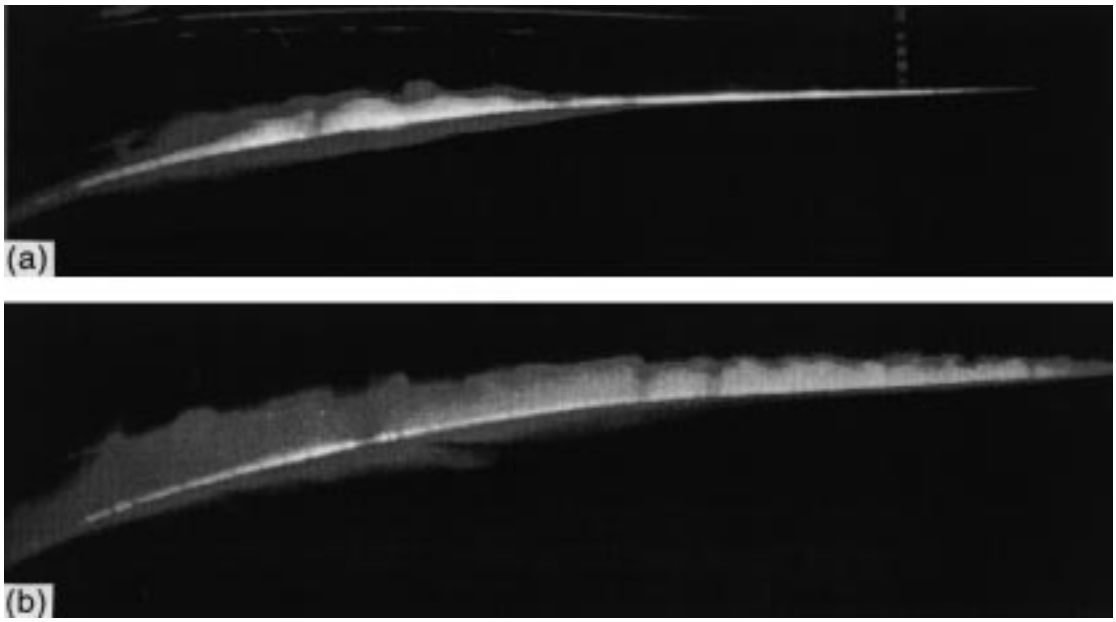

Fig. 3. (a) Laminar-turbulent transition on the smooth surface; (b) Turbulent boundary layer on rough surface.

present investigation, in the straight section of the tunnel with zero pressure gradient. In Fig. 6a, the dimensionless distance from the wall is the abscissa and to determine the friction velocity in this parameter, as well as the dimensionless mainstream velocities, the stationary values of the Reynolds stresses near the wall in Fig. 5 were used. The figure also presents some results for fully rough flow over surfaces of closely packed spheres reported by Ligrani and Moffat [7]. Their velocity distributions compare well with those of the present investigation in the log-law region. Differences between the present data and those of [7] are accountable by the different degrees of boundary layer development in the two investigations, represented by the respective momentum thickness Reynolds numbers. For the results plotted from the present investigation, this parameter was about 4000, compared with over 9000 in [7]. Both sets of results demonstrate the typical increase in slope of the velocity as the distance from the rough wall increases: the same effect is seen with the smooth wall data of the present work. Here too, the agreement with the normal smooth wall velocity distribution, shown as the full line, is as expected, good only in the log-law region near the laminar sublayer.

Fig. 6b shows the dimensionless velocity distribution with the wall distance normalised with respect to the element height on the rough wall. The full line has a slope of 2.5 on these ordinates, as is usually assumed for commercially rough surfaces. Again, the fit with the experimental observations is satisfactory only near the sublayer and the intercept on the abscissa at $\log_e(y/k) = 0$ is about $U/U^* = 8$.

Table 1 summarises the test conditions for this whole programme for which the determination of heat transfer rates had the highest priority. Thus, detailed measurements of the fluid dynamic conditions were restricted to the smooth surface and the rough surface with elements 1 mm in height. Some of the parameters for the remaining two surfaces have been estimated by interpolation between observed results (these are indicated with an asterisk in the table and when referred to elsewhere in the paper).

The data in this paper are given as averaged samples to show general trends. All the results along the whole length of the tunnel, plotted and tabulated in full for fluid dynamic and heat transfer tests, are available and presented by Hubbe-Walker [8].

3.3. Heat transfer

Measurements of heat transfer were made over a wider range of flow conditions than in the fluid dynamic programme. Further, the height of the roughness elements was successively reduced by machining from 1 to 0.75 mm and then to 0.5 mm to compare the performance of the consequent different roughness levels on the surface. The apparatus was carefully calibrated for heat loss from the element bars so that the flux could be determined from measurements of electrical power. The heating control system linked to the thermistors in the aluminium bars ensured, that the surface temperature was kept constant throughout the

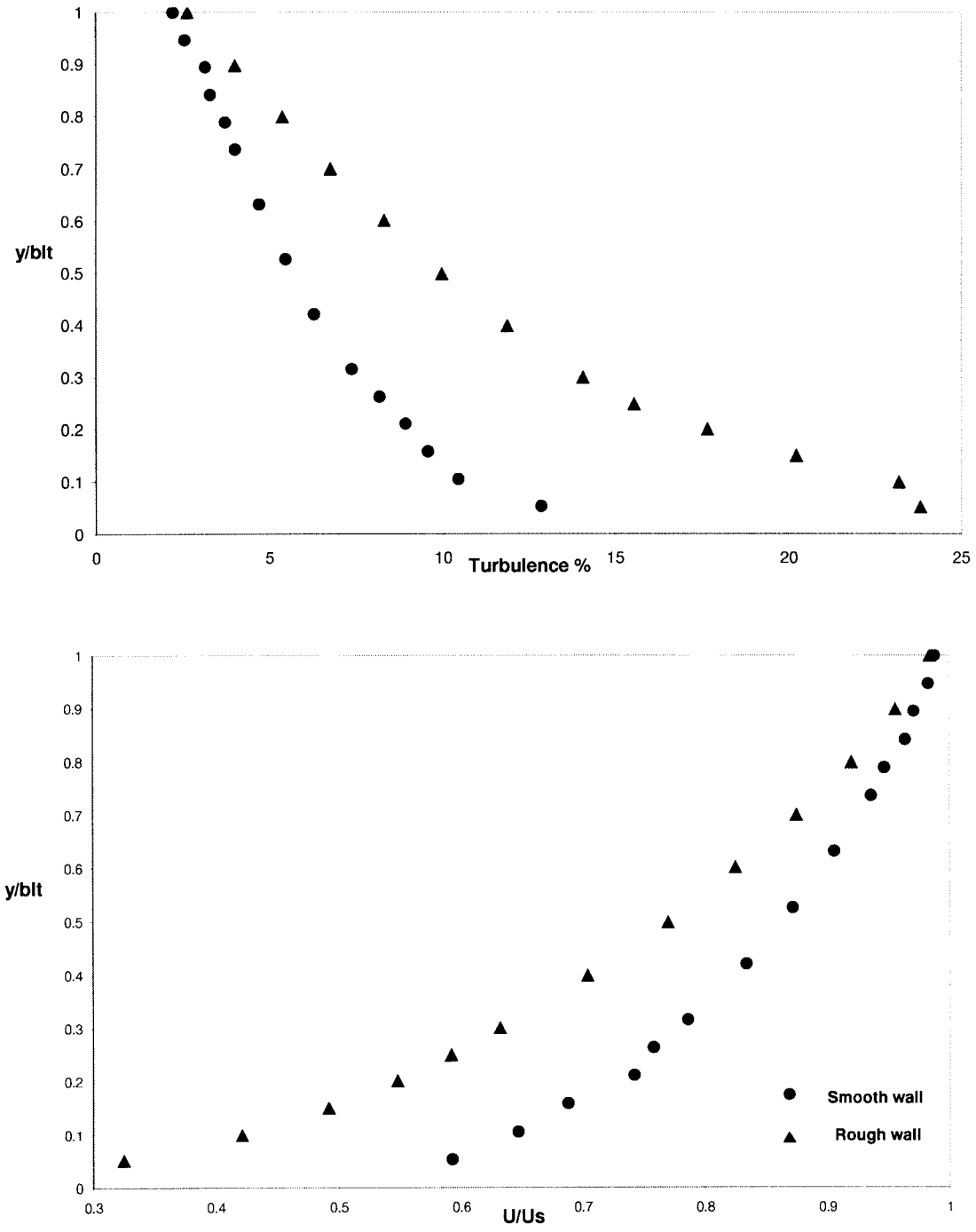

Fig. 4. Streamwise velocity and turbulence intensity on the rough and smooth surfaces at 330 mm, $U_s = 22.0$ m/s (blt = boundary layer thickness).

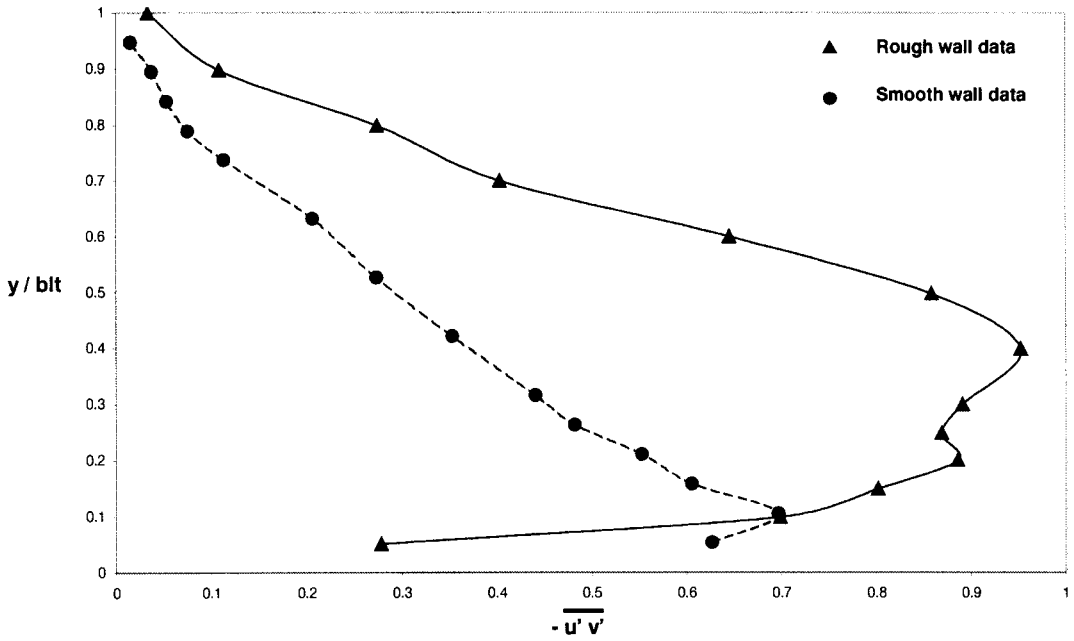

Fig. 5. Reynolds shear stress in the boundary layer (m^2/s^2).

test series at 30°C under strict and often time-consuming thermal equilibrium conditions along the working section. The freestream temperature was taken as the total value determined just upstream of the test section. The recovery temperature commonly used to define the controlling temperature difference for heat transfer over a surface was not used, since the recovery factor is known to be a function of the roughness levels, although for the conditions used here, there is comparatively little difference.

The variation of heat transfer coefficient along the surface was essentially monotonic, apart from two or three of the most upstream and downstream readings. Here, there was evidence for the former of occasional separation that led to a reduced coefficient that rose again on reattachment. The conduction heat loss determinations were also slightly less reliable in both areas. With these exceptions, the coefficients were observed to fall consistently as about the 0.2 power of the distance along the surface, as is usual for turbulent flow on smooth and rough surfaces. As will be seen, the coefficients also fell, as reducing the height of the elements decreased the roughness of the wall.

Relatively little change in heat transfer rate is ex-

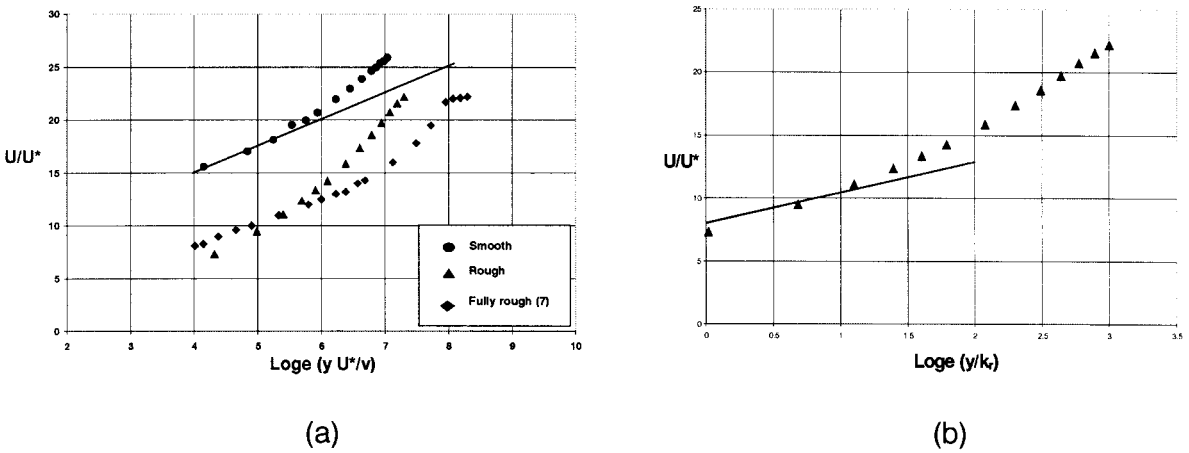

Fig. 6. Non-dimensional velocity distributions.

Table 1
Summary of the test conditions

Surface	Smooth	Rough	Rough	Rough
Element height (mm)	0	1.0	0.75	0.5
Mainstream velocities (m/s), LDA measurements	22.0	21.7–22.4	–	–
Mainstream velocities (m/s), heat transfer tests	22	17.0–40.0	17.0–40.0	17.0–40.0
Mainstream turbulence intensity (%)	2.2	2.6	2.5*	2.4*
Pressure gradient parameter $(\nu/U_s^2)\,dU_s/dx, \times 10^7$	0	−1.3 to +1.5	−1.3 to +1.5	−1.3 to +1.5
$1/n$ at $x = 300$ mm (average)	5.3	2.65	–	–
Boundary layer thickness at $x = 300$ mm (average)	19.0	20.0	–	–
Friction velocity, U_τ (m/s)	0.84	0.97	0.90*	0.83*
Roughness Reynolds number	0	69	46*	29*

hibited as the test section changes from straight to curved. If the heat transfer coefficients of Fig. 7 are plotted on logarithmic co-ordinates separately for the two regions, there is a small reduction in the slope between the straight and curved sections of the tunnel, corresponding to an increase in heat transfer of only between 2 and 3% at the end of the tunnel due to the curvature, compared with an equivalent straight section. This observation is consistent with the observations of Ligrani and Hedlund [9] who show similarly small changes on the convex surface of a bend at comparable curvatures but in a tripped turbulent flow at lower Reynolds and Dean numbers, than here.

The effects of pressure gradients in the flow are also shown in Fig. 7, in which are plotted the heat transfer coefficients on the surface of intermediate roughness, i.e., the element heights machined down to 0.75 mm. The results are for two inlet velocities, 22 and 40 m/s which, for one set, was unchanged along the test section. In the other, the tunnel roof was set to accelerate the flow to give an outlet velocity of 30.4 and 43.8 m/s, respectively. In extensive programmes of research at Stanford and Mississippi State Universities, using surface roughness generated by regularly spaced attached hemispheres [10,11], an acceleration parameter, $K_r = (k_r/U_s)(dU_s/dx)$, was developed for application to rough surfaces. In this work, the radius of the hemispheres was taken as the dimension k_r. In the present work, using the height of the elements gives K_r as 0.00029, as shown in Fig. 7. The corresponding acceleration parameter used for flows over turbine blades $(\nu/U_s^2)(dU_s/dx)$, has a value of about 1.5×10^{-7}, a factor of 10 or more below the values expected significantly to affect such flows. The acceleration in the present flows leads, for the lower velocity, to an increase in heat transfer coefficient of about 18%, and rather less at the higher velocity. A negative velocity gradient applied in the upstream half of the straight

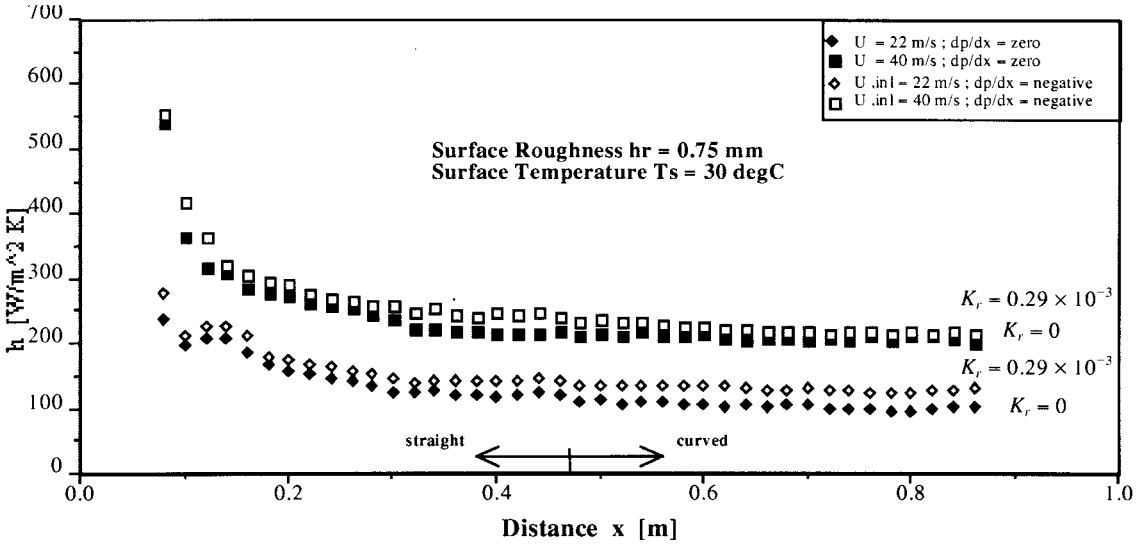

Fig. 7. Heat transfer coefficients for zero and negative pressure gradient ($Re_k = 46^*$).

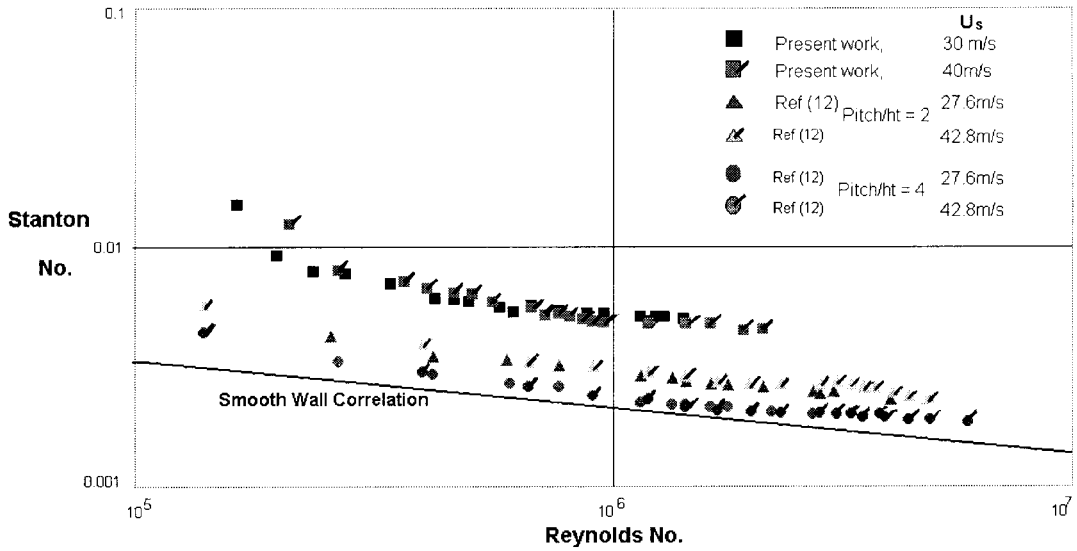

Fig. 8. Stanton number vs. Reynolds number for 1 mm roughness ($Re_k = 69$), compared with data from [12] ($Re_k = 8$ and 70) and the smooth wall correlation.

wall appeared to have little effect on the measured heat transfer rates, as might have been anticipated in the absence of any tendency toward separation of the flow.

The dimensionless plot of Fig. 8 shows the Stanton numbers for zero pressure gradient, as a function of the surface Reynolds number calculated from the leading edge, for the two highest velocities of the present experiments and the highest, 1 mm, roughness. These are compared with the corresponding standard smooth wall correlation and some results at comparable velocities from those reported by Hosni et al. from the Mississippi programme [12] with hemispherical roughness elements. It is relevant to observe that for Hosni's hemispheres, according to the method of Schlichting [13], the equivalent sand roughness is 0.10 mm for the more widely pitched elements and 0.63 for those pitched more closely. For the former, where the roughness Reynolds number Re_k is about 8, the heat transfer rates are very close to the smooth correlation. For the latter, Re_k at about 70 is well into the fully rough region, the onset of which can be as low as 55 for hemispherical roughness according to Ligrani and Moffat [7], and the heat transfer is appreciably greater. For the present work, using the dimensionless velocity plot of Fig. 6b with the abscissa y/k_s, the intersection on the ordinate was seen to be about 8, giving, according to Schlichting, an equivalent sand roughness height of 1.09 times the element height and corresponding roughness Reynolds numbers of about 70. Although it is also reported in [7] that fully rough onset Reynolds numbers as high as 90 can be associated with non-spherical roughness elements as in the present work, the heat transfer coefficients of Fig. 8, being more than 70% greater than with the hemispheres of Hosni [12], suggest that these flows are also in the 'fully rough' regime.

Fig. 9a and b are further dimensionless plots to show separately the results from the present programme from the tests with a zero pressure gradient and the two reduced roughness heights, 0.75 and 0.5 mm — the latter value being comparable to the roughness of the eroded turbine blade of Fig. 1. The previously observed effects of curvature and pressure gradient have been seen to be small compared to the changes in heat transfer rate produced by the roughness, as this figure confirms. The heat transfer rates observed here show a tendency to collapse towards a single line at the highest Reynolds numbers. The asymptotic value of the corresponding Stanton number is about 0.0051 for the 1 mm high roughness, 0.0043 for the 0.75 mm height and 0.0035 for the lowest, 0.5 mm height. This result correlates as a nearly linear function of limiting value against roughness, with the extrapolated zero value equivalent to the 'smooth' surface prediction at a Reynolds number of about 2×10^6. Hosni's [12] data in Fig. 8 show a similar but less pronounced trend. Note also that his fully rough data, represented approximately as the dashed line, closely match the results from the 0.5 mm high elements in the present work even though the corresponding roughness Reynolds number is estimated to be lower here and in the centre of the usually accepted transition range.

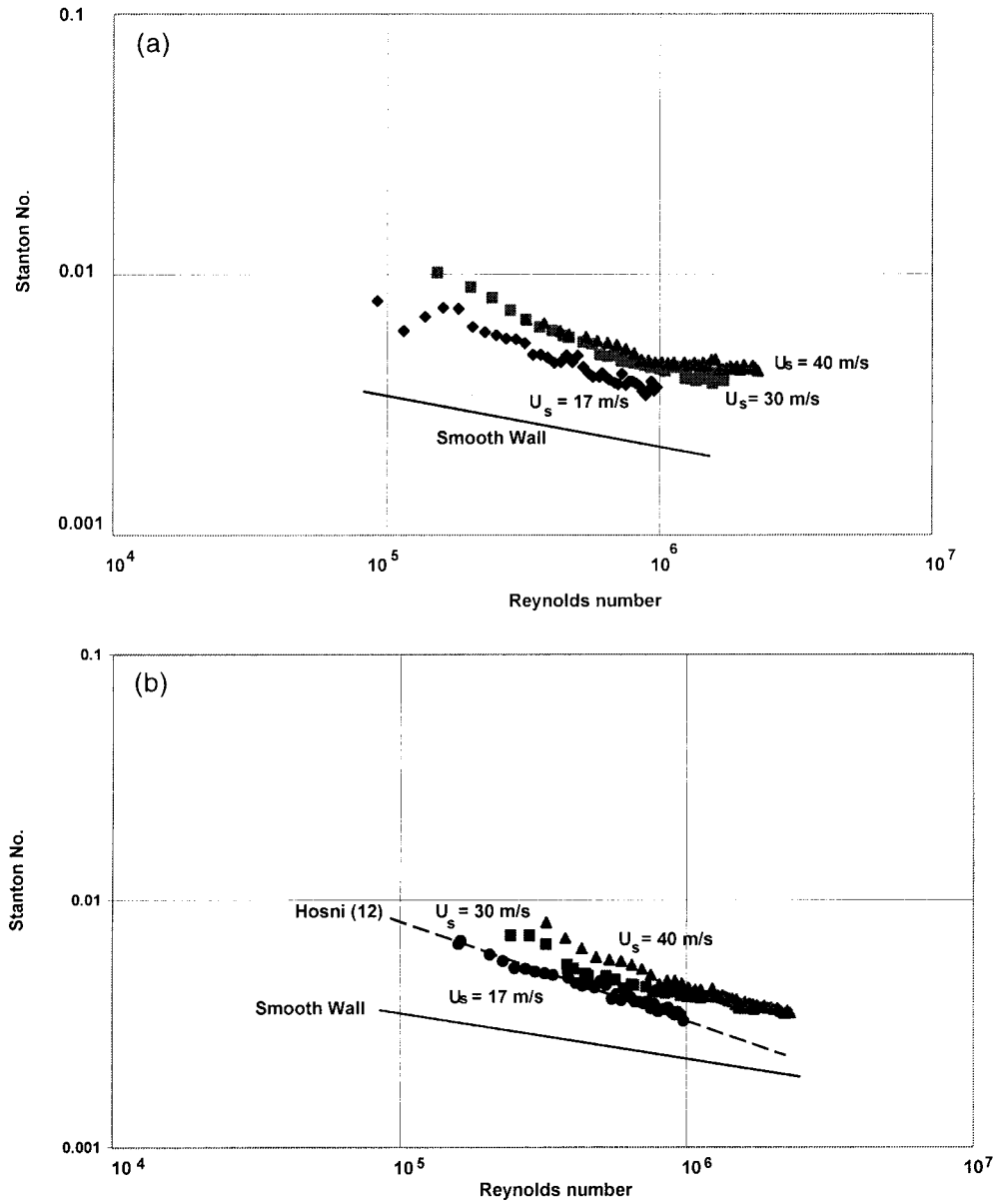

Fig. 9. Stanton number vs. Reynolds number in zero pressure gradient for roughness heights: (a) 0.75 mm ($Re_k = 46^*$) and (b) 0.5 mm ($Re_k = 29^*$).

4. Theoretical predictions of heat transfer on rough surfaces

Reference was made earlier to the work in the authors' laboratory to develop a theoretical CFD procedure for predicting heat transfer rates over rough surfaces, curved or straight, in variable pressure gradients. Validation of this theory [1,4] was declared as a major object of the present experimental programme. The theory is two-dimensional and uses an algebraic stress model following Jones and Launder [5], modified for surface curvature effects and employing the basic philosophy for roughness modelling developed originally by Coleman [10]. Ten equations are used to define the flow, three for streamwise momentum, two for stagnation enthalpy, two for turbulent kinetic energy, two for turbulent dissipation and one for transverse momentum equation. The theory is thus referred to as

TEN and the definitions of parameters to represent the geometry of the surface roughness and their effect upon the turbulence parameters are its key.

The fluid dynamic consequences of surface roughness arise from the 'blocking' effect of the roughness elements in reducing the area for flow between them, so creating frequent velocity changes with consequent wakes in the fluid near the wall. An average blocking factor can be calculated for any form of roughness if the variation of width with height from the base surface is known, as for the structured pyramidal and trapezoidal forms used in the present work. Two such parameters were defined for TEN — an average value derived by integrating in the three co-ordinate directions and an approach value defined by the frontal area of the elements.

The topography is used to modify both the specific kinetic energy of turbulence, k in the algebraic stress model, and the turbulent dissipation term, ε. By considering the action of the roughness elements in creating wakes with enhanced turbulence and decelerating the fluid by form and skin friction drag, positive and negative source terms can be hypothesised, producing a net effect that represents a small difference between two much larger quantities. What is in effect an extension of the classical turbulence closure problem thus requires an empirical input for the resultant turbulence modifying terms. Examination of the earlier experimental work at Stanford and Mississippi [10,11] enabled Tarada [1,4] to determine the modifications which gave the best agreement with the observed results of the fluid flows and resultant heat transfer.

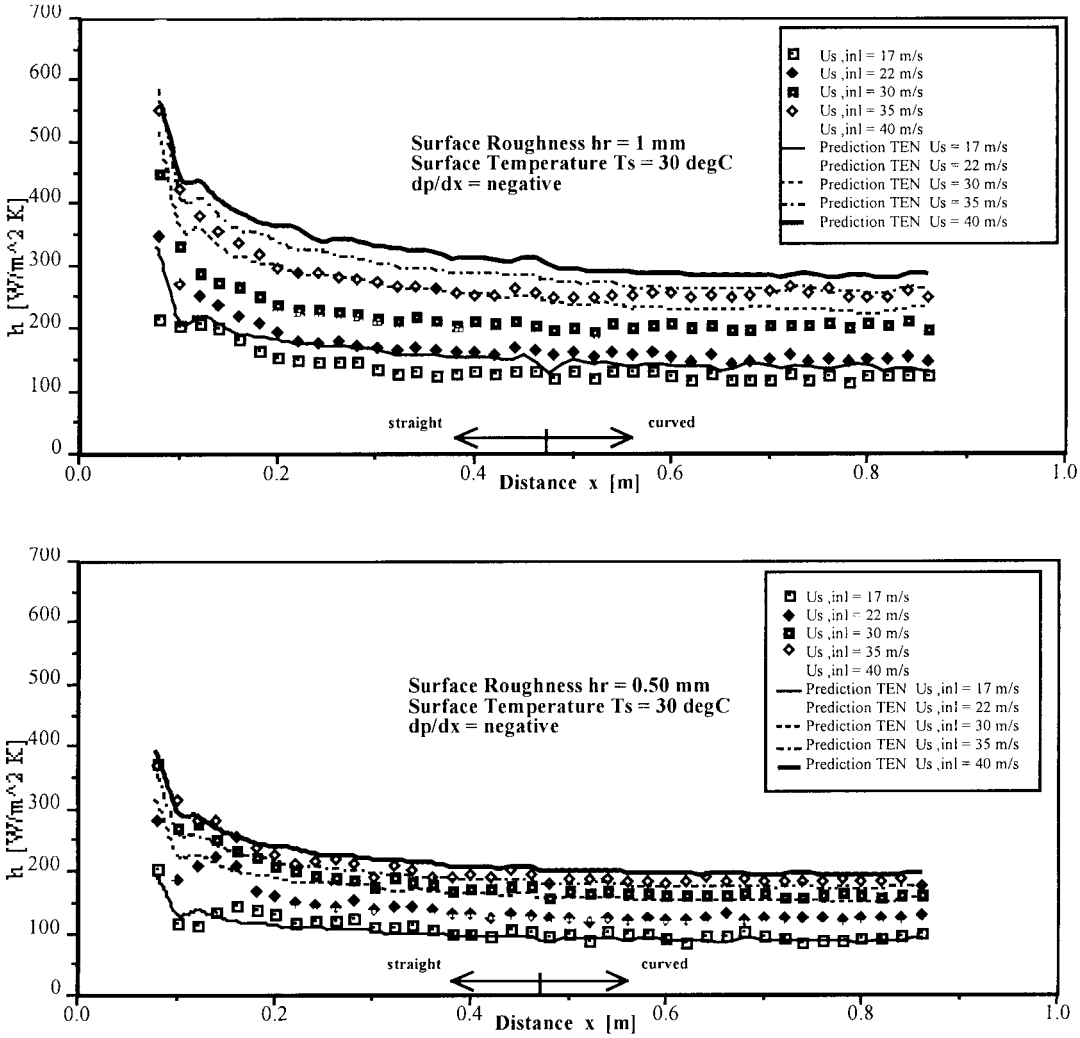

Fig. 10. Comparison of measured heat transfer coefficients on two of the rough surfaces (1 mm and 0.5 mm, $Re_k = 69$ and 29*) and the theoretical predictions [1,4].

Obtaining stable and convergent numerical solutions of the resulting equations required considerable further adaptation of the flow and geometric parameters. In particular, at the base of the roughness elements the blockage ratio is effectively unity, so that the throughway is locally zero. This value led to instabilities in the computer programme that could only be resolved by notionally moving the elements apart. The separation distance was used to define a 'ramping factor' as a fraction of the pitch of the elements. Its value affected the flow over a surface by altering the roughness but a value of 0.1 was found to be the optimum, both computationally and in predicting the observed results.

Fig. 10 compares Tarada's predictions of heat transfer coefficients with experimental measurements on the roughest and least rough surfaces tested in this work. Although differences between prediction and observation are usually within the experimental uncertainties, the figure shows that there is a tendency to overpredict the heat transfer coefficients by up to 10% at the highest velocity tested on the rougher surfaces—a similar effect was observed with a zero pressure gradient. A general and possibly more significant comment applies for the curved surface. For this, the code predicts a small step downward change in coefficient not observable in any of the tests. Generally, however, Fig. 10 demonstrates that the predictions of Tarada's code, certainly in predicting the gross effects of roughness with the parameters previously described, are in fair to good agreement with the observations from the flow conditions tested here.

5. Summary and conclusions

This paper describes a programme of research to examine the fluid flow and heat transfer over a wide range of conditions on surfaces with structured roughness. A selection of the observed results is presented and the complete set are available as reference [8]. The experimental observations are compared with those from other relevant investigations but, in particular, the object of the present paper has been to determine how these observations are predicted by the analysis developed in the authors' laboratory specifically for rough surfaces which occur commonly in real engineering applications [1,4].

Surface curvature and velocity gradients in the ranges of Dean number and acceleration parameter used in the present work had relatively little effect on heat transfer, as compared to the roughness. Curvature appeared to cause an increase of 2 to 3% compared with the comparable straight section. A positive velocity gradient showed increases in heat transfer up to 18% at the lower mainstream velocities tested, albeit at an acceleration parameter, a factor of 10 or so lower than commonly found in turbine practice.

The pyramidal elements employed, showed the long established enhancement of heat transfer by the turbulence generated by the roughness and this was over 70% at comparable values of the roughness Reynolds number than observed under comparable conditions for the spherical forms commonly used by other workers [10–12].

Although the CFD code [1,4] used for comparison tends to overpredict heat transfer rates by up to 10% at the highest velocities, discrepancies are usually within the experimental uncertainties and there is fair to good agreement with the gross effects of the roughness.

References

[1] F.H.A. Tarada, Heat transfer to rough turbine blading. University of Sussex, D.Phil thesis, 1987.
[2] J. Nikuradse, Strömungsgezetze in rauhen Rohren. Forschg. Arb. Ing.-Wes. No. 361, 1933.
[3] A.B Turner, F.H.A. Tarada, F.J. Bayley, Effect of surface roughness on heat transfer to turbine blades. AGARD Conference. Heat Transfer and Cooling in Gas Turbines. AGARD-CP-390, 1985.
[4] F.H.A. Tarada, M. Suzuki, External heat transfer enhancement to turbine blading due to surface roughness. Paper no. 93-GT-74, ASME Gas Turbine Conference, 1993.
[5] W.P. Jones, B.E. Launder, The prediction of laminarisation with a two-equation model of turbulence, Int. Journal of Heat and Mass Transfer 15 (1972) 301–314.
[6] C. Tropea, A note concerning the use of a one-component LDA to measure shear stress terms, Experiments in Fluids 1 (1983) 209–210.
[7] P.M. Ligrani, R.J. Moffat, Structure of transitionally rough and fully rough turbulent boundary layers, J. Fluid Mech 162 (1986) 69–98.
[8] S.E. Hubbe-Walker, An experimental study of the effects of roughness and curvature on heat transfer in turbulent boundary layers. University of Sussex, D.Phil. thesis, 1996.
[9] C.R. Hedlund, P.M. Ligrani, Heat transfer in curved and straight channels with transitional flow, Int. Journal of Heat and Mass Transfer 41 (3) (1998) 563–573.
[10] H.W. Coleman, R.J. Moffat, W.M. Kays, Momentum and energy transport in the accelerated fully rough boundary layer. Stanford University Report No. HMT-24, 1981.
[11] H.W. Coleman, Generalised roughness effects on turbulent boundary layer heat transfer. Mississippi State University Report MSSU-TFD-84-1, 1983.
[12] M.H. Hosni, H.W. Coleman, R.P. Taylor, Measurements and calculation of rough wall heat transfer in the turbulent boundary layer, Int. Journal of Heat and Mass Transfer 34 (4/5) (1991) 1067–1082.
[13] H. Schlichting, in: Boundary-Layer Theory, 6th ed, McGraw-Hill, New York, 1968, pp. 586, 587, 610–622.